International Journal of Robotics and Control Systems
Vol. 6, No. 1, 2026, pp. 495-506
ISSN 2775-2658
http://pubs2.ascee.org/index.php/ijrcs

Sliding Mode Control Based Whale Optimization Algorithm for Duffing Oscillator

Mohammed K. Hamzah [a,1], Laith K. Majeed [a,2], Ahmed S. Al-Araji [a,3], Hussien Dulaimi [a,4,*], Huthaifa Al-Khazraji [a,5]

[a] College of Artificial Intelligence Engineering, University of Technology-Iraq, Baghdad, Iraq
[1] 60115@uotechnology.edu.iq; [2] laith.k.majeed@uotechnology.edu.iq; [3] 60166@uotechnology.edu.iq;
[4] hussein.s.mohammed@uotechnology.edu.iq; [5] huthaifa.k.ibrahim@uotechnology.edu.iq
* Corresponding Author

ARTICLE INFO

Article history
Received December 20, 2025
Revised January 14, 2025
Accepted February 12, 2026

Keywords
Duffing Oscillator;
Sliding Mode Control;
Whale Optimization Algorithm;
MATLAB-Based Simulations

ABSTRACT

The Duffing oscillator is particularly useful in numerous applications, owing to its unique dynamic features. It integrates a periodically excited system with a nonlinear elastic restoring force. This paper proposes a sliding mode control (SMC) for trajectory tracking of the Duffing oscillator. To guarantee best dynamic performance of the SMC, two reaching laws are examined. The first reaching law of the SMC is based on the hyperbolic tangent function (SMC_{tah}) whereas the second one is based on the saturation function (SMC_{sat}). The design parameters of the proposed controllers are optimized through tuning with the whale optimization algorithm (WOA) to achieve enhanced performance. Extensive MATLAB-based simulations were carried out to confirm the effectiveness of the proposed approaches. The simulation outcomes reveal that the tracking error based on the integral of absolute error (IAE) of the system controlled by the SMC_{tah} is reduced by 8.6% compared to that of the system controlled by the SMC_{sat}. Furthermore, under uncertainty scenario, SMC_{sat} shows more robustness than SMC_{tah}.

1. Introduction

Sliding Mode Control (SMC) has traditionally been viewed as a powerful and effective nonlinear control approach, and it is especially practical in dealing with those systems that are exposed to modeling uncertainties and external disturbances [1]–[3]. It was conceived in the late fifties in the Soviet Union by seminal publications of Emelyanov and formalized by Utkin. This initial work presented a control infrastructure with the ability to maintain the desired system behavior even within large parameter variation [4], [5]. In further decades, SMC has developed as a flexible paradigm, whose force is enhanced by the property of intrinsic invariance and the relative simplicity of the implementation of the system as soon as the system reaches the identified sliding surface [6].

In the literature, SMC has been applied across all of mechanical, electrical, automotive, and aerospace systems, as an influential tool that can be trusted to provide a good nonlinear control strategy. For example, SMC has been used to stabilize intrinsically unstable behavior of the

levitation system and achieve accurate position control during the occurrence of model errors and system parameter variations, reported in academic papers [7], [8]. The SMC has also been applied to non-linear mechanical systems such as the propeller pendulum where it has been shown to be both reliable in tracking performance and resilient to external perturbations [9]. SMC has also been used to success in the renewable energy industry, especially towards photovoltaic (PV) systems in order to maintain a steady operation and efficient maximum power point tracking of the system in speedily changing environmental conditions [10]. In addition to these applications, SMC has also been widely studied and used in some of the key fields of control engineering. SMC has been commonly used in robotics, especially in manipulators, to compensate severe nonlinear behavior, payload dynamics, unmodeled joint friction, helping to achieve exact tracking of the trajectory and disturbance rejection using multi degree-of-freedom structures [11]. Inverted pendulum systems representing characteristic examples of underactuated systems and unstable nonlinear plants have shown that SMC can provide effective control of the system in stabilizing the system to reference and track a goal value despite various versus a number of parametric uncertainties and external perturbations [12]. In the ambit of electric motor drives, the SMC has been used to control speed and ride in DC, and AC machine, and hence offer quick dynamic reaction and load resilience with respect to disturbance oscillations and changes in electrical characteristics [13]. Similarly, automotive suspension systems have enjoyed the advantages of SMC, and it was applied to improve the ride comfort and road performance by strongly compensating nonlinear suspension behavior and externally caused excitations posed by irregular road surfaces [14]. SMC has also been accepted in the aerospace and aerial robotics field with the use of unmanned aerial vehicles to compete with the nonlinear rich aircraft dynamics, external forces such as wind gusts, and the model error so as to maintain stable attitude and trajectory control [15]. Moreover, SMC has been broadly applied to mobile robot systems, and it has allowed strong motion control and path following behavior in the presence of uncertainties in the wheel-ground contact, the actuator dynamics and external disturbances [16].

In spite of its numerous advantages, classical SMC formulations are encountering a stubborn problem of high-frequency fluctuations called chattering that is mainly caused by the high-frequency nature of the discontinuity of the control law [17]. This does not only worsen the performance of the system but can also arouse unmodeled dynamics or stress on a real work implementation. Therefore, much has been done on optimization of reaching step to achieve faster convergence, greater strength, and reduced chattering [18], [19]. It is important to note that reaching based approaches have recently gained significant attention because of the ability to explicitly control the dynamic of the sliding variable before the attainment of the sliding manifold, and so provide designers with more flexibility in balancing the behavior during the transient convergence as well as steady-state behavior, which subsequently provides better stability and smoother operation. It is based on the classical laws of SMC that more advanced laws of continuous reaching have been suggested in recent studies that enable quick, regulated convergence and that efficiently suppress chattering when in the immediate surroundings of the sliding surface. Such developments support the fact that sliding mode control is still relevant to state-of-the-art control engineering and that it is highly adaptable when it comes to modern control design [20].

Building upon insights from prior studies and motivated by the exploration of alternative application of SMC, this paper proposes a SMC for trajectory-tracking for a Duffing oscillator. The Duffing oscillator holds significant importance because it embedded essential characteristics of nonlinear dynamics that linear models fail to capture. In contrast to the simple harmonic oscillator, it incorporates a nonlinear stiffness term, making it a foundational benchmark for investigating real-world nonlinear phenomena. For the purpose of examination of the performance of different structure of the SMC, two reaching law in this paper are considered. Specifically, the hyperbolic tangent–based reaching law (SMC_{tah}) and the saturation-based reaching law (SMC_{sat}) are implemented. Whale optimization algorithm (WOA) is a metaheuristic optimization method well-known for its good balance between exploration and exploitation. Moreover, it does not require gradient information and needs few control parameters. Therefore, the parameters of the proposed control schemes are optimized via WOA for performance improvement.

2. Duffing Oscillator

Duffing oscillator is a typical nonlinear second-order differential equation, which can reflect many nonlinear intrinsic phenomena. Thanks to its well-defined mathematical structure and complex nonlinear behavior, the Duffing oscillator is commonly used as a benchmark for analyzing nonlinear vibrations, investigating chaos, and evaluating nonlinear control and identification strategies [21]. The following mathematical equation is the system model of the Duffing oscillator [22].

$$\ddot{x} + c\dot{x} + bx^3 = A\,cos(t) \tag{1}$$

In this expression, c represents the damping coefficient, that is, the magnitude of dissipative influences. The degree of nonlinearity in the restoring force is measured by the parameter b. The amplitude of the periodic driving force is determined by the constant A. These constant terms are very crucial in influencing the system dynamics; their changes vary the qualitative behavior of the model. The equation simplifies to the equations of a damped, driven simple harmonic oscillator when the γ value is zero and that of the system is driven when A is set to zero. The equation of Duffing (1) is also can be written as follows:

$$\dot{x}_1 = x_2 \tag{2}$$

$$\dot{x}_2 = -cx_2 - bx_1^3 + A\,cos(t) + u \tag{3}$$

Hence, x_1 represents the position x, x_2 represents the velocity ẋ and u represents the control input. In the purpose of designing the SMC controller in the next section, (3) can be further rearranged as follows:

$$\dot{x}_2 = F(x,t) + u \tag{4}$$

where

$$F(x,t) = -\alpha x_2 - \gamma x_1^3 + A\,cos(t) \tag{5}$$

3. Sliding Mode Control Design

The incorporation of a feedback controller enhances system performance. Therefore, it has been applied for a wide range of systems [23]–[31]. Sliding mode control (SMC) is a recognized durable and methodical designing controller. It has two phases. The first phase is to define the surfaces that slide such that they meet the performance requirements. The next phase involves maintaining the system on the sliding surface [32], [33]. The procedure to design the control law of the SMC can be stated as follows.

Define the tracking error as:

$$e = x_d - x_1 \tag{6}$$

where x_1 is angular position output and x_d is the desired angular position. Taking the first derivative of e yields:

$$\dot{e} = \dot{x}_d - \dot{x}_1 = \dot{x}_d - x_2 \tag{7}$$

Taking the second derivative of e yields:

$$\ddot{e} = \ddot{x}_d - \dot{x}_2 \tag{8}$$

Substitute $\dot{x}_2$ from (5) into (8) obtains:

$$\ddot{e} = \ddot{x}_d - F(x,t) - u \tag{9}$$

The sliding surface is selected as follows:

$$s = \dot{e} + a_{smc}e \tag{10}$$

where $a_{smc} > 0$ is the tuning parameters.

The application of the first derivation of the sliding surface leads to:

$$\dot{s} = \ddot{x}_d - F(x,t) - u + a_{smc}\dot{e} \tag{11}$$

The second part of the SMC control law is the reaching law (RL). RL drives the system to slide along a predefined surface. For the system to stay on this surface, the derivative of the sliding surface must match the selected RL. Therefore, selecting an appropriate RL is crucial to minimize the chattering effect commonly associated with SMC. In this study, two RLs are proposed to address this issue. The first RL is based on the hyperbolic tangent (tanh) function and is given by [34], [35]:

$$\dot{s} = -k_{tah}\, tanh(s) \tag{12}$$

Where k_{tah} is a tuning parameter, which is a strictly should be positive number, where $tanh\, s$ is given by

$$tanh\, s = \frac{e^s - e^{-s}}{e^s + e^{-s}} \tag{13}$$

Based on this RL, the control u_{tah} is obtained by setting (12) is equal to (11) and accordingly the (14) is obtained as follows:

$$\ddot{x}_d - F(x,t) - u_{tah} + a_{tah}\dot{e} = -k_{tah}\, tanh(s) \tag{14}$$

Rearrange (14) to find u_{tah}:

$$u_{tah} = \ddot{x}_d - F(x,t) + a_{tah}\dot{e} + k_{tah}\, tanh(s) \tag{15}$$

The second RL is based on the saturation (sat) function and it is given by [36], [37]:

$$\dot{s} = -k_{sat}sat(s/\emptyset) \tag{16}$$

where k_{sat} is adjusted parameter > 0, $sat(s/\emptyset)$ is given by:

$$\text{sat}\left(\frac{s}{\emptyset}\right) = \begin{cases} +1 & \text{if } \frac{s}{\emptyset} > 0 \\ \frac{s}{\emptyset} & \text{if } -1 < \frac{s}{\emptyset} < 1 \\ -1 & \text{if } \frac{s}{\emptyset} < 0 \end{cases} \tag{17}$$

The control law for this RL u_{sat} is given by putting (16) and is equal to (11) as given:

$$\ddot{x}_d - f(X) - bu_{sat} + a_{sat}\dot{e} = -k_{sat}sat(s/\emptyset) \tag{18}$$

Rearrange (18) to find u_{BL}:

$$u_{sat} = \ddot{x}_d - F(x,t) + a_{sat}\dot{e} + k_{sat}sat\left(\frac{s}{\emptyset}\right) \tag{19}$$

4. Whale Optimization Algorithm

Swarm optimization techniques are characterized by iterative and probabilistic search mechanisms that enable efficient handling of complex optimization problems [38]–[42]. These

algorithms provide generic, domain-independent problem solving strategies, as contrasted to traditional optimization strategies which are based upon a problem-specific domain-specific expertise [43]. Moreover, these methods are designed as based on the phenomena of social interactions, nature, and different paradigmatic approaches to problem solving. As a result, a substantial body of research has introduced diverse swarm-based algorithms aimed at optimizing the design parameters of different control systems [44]–[46]. In this regard, whale optimization algorithm (WOA) was presented by Mirjalili and Lewis [47], which is based on the foraging behavior of humpback whales. In the literature, it has been demonstrated that this algorithm can effectively address a broad class of optimization problems and exhibits superior performance compared to existing methods. For example, WOA has been applied to train the weights and biases of artificial neural networks [48], solve the resource allocation problems in wireless networks [49], solve the maximum flow problem [50], and optimize ship path optimization under complex marine environment [51].

The algorithm is organized to have three different sub-models namely prey search, spiraling bubble-net feeding, and prey encirclement. The pseudo-code related to the WOA is shown Fig. 1. When humpback whales spot the position of the prey, which can be compared to the identification of the position of the most desirable agent, they can position around the prey using two simultaneous approaches. The first one is called the shrinking circle, which drives the population of whales (i.e. the remaining the agents) to revise their current positions near the optimal search agent. The mathematical equation used in this situation is the following [52]:

$$H_w = |D_w P^* - P_i(itr)| \tag{20}$$

$$P_i(itr+1) = P^* - (F_w H_w) \tag{21}$$

1. **Input**
   - Objective function, Population size (N), Number of iteration (T_{max})
2. **Initialization**
   - Initialize population N
   - Evaluate objective function
   - Assign P^*
3. **Loop:**
   - while (itr < T_{max})
     - For each search agent
       - ✓ Update a_w, F_w, D_w, l_w and ρ
       - ✓ If ρ > 0.5
         - ➢ If $|F_w| < 1$
           - ❖ Generate a new solution based on Eq. (20) and Eq. (21)
         - ➢ If $|F_w| \geq 1$
           - ❖ Select a random search agent P_{rand}
           - ❖ Generate new solution based on Eq. (27) and Eq. (28)
       - ✓ If ρ ≤ 0.5
         - ➢ Generate new solution based on Eq. (25) and Eq. (26)
     - Perform greedy selection and update P^*
     - itr = itr + 1
   - end while
4. **Print the Optimal Solution**

Fig. 1. WOA's pseudo-code

The coefficients F_w and D_w are computed as follows:

$$F_w = 2a_w r_1 - a_w \tag{22}$$

$$D_w = 2r_2 \tag{23}$$

where, i, itr indicate the iteration and agent respectively. The parameters of current and nested solution are represented by the parameters $P_i(itr)$ and $P_i(itr+1)$, respectively. The optimal solution is denoted as P^* and a_w is a line decreasing coefficient of 2 to 0. Both coefficients r_1, r_2 are random numbers that lie in the range [0.1]. The second method of movement is spiral in nature. The humpback whale movement in this mode is characterized in the following manner [53].

$$\acute{H}_w = |P^* - P(itr)| \tag{24}$$

$$P_i(itr+1) = P^* + \left(\acute{H}_w e^{b_w l_w} cos(2\pi l_w)\right) \tag{25}$$

In which the coefficient b_w controls the width of the whale in a logarithmic spiral motion and l_w is a random number between the range of -1 and 1. In order to maintain the right equilibrium between the spiral mode and the shrinking encircling mode, a 50% chance of either the mode being chosen is assumed. This process is formulated as follows [54]:

$$P_i(itr+1) = \begin{cases} P^* - (F_w H_w) & \rho > 0.5 \\ P^* + \left(\acute{H}_w e^{b_w l_w} cos(2\pi l_w)\right) & \rho \leq 0.5 \end{cases} \tag{26}$$

In which case, we can also consider the random real number, where the values lie in the range [0,1], denoted by ρ.

In the process of exploration, humpback whales hunt at random. Instead of using an optimal placement of the whale, the case is controlled by the position of a randomly chosen agent in the group in this step. This is the case when $|F_w| \geq 1$. The mathematical model of this process is given by:

$$H_w = |D_w P_{rand} - P_i(t)| \tag{27}$$

$$P_i(t+1) = P_{rand} - (F_w \times H_w) \tag{28}$$

where, P_{rand} is a random place among the members of the population.

5. Simulation and Result

To evaluate the proposed, optimize SMC for Duffing oscillator, a computer-based-simulation was carried out using MATLAB software. The numerical value of the Duffing oscillator is listed Table 1. The cost function used by the WOA namely the integral of absolute error (IAE) was identified to achieve optimal performance of SMC_{tah} and SMC_{sat}.

Table 1. Parameters of Duffing oscillator

Parameters	Value
c	0.1
b	1
A	12

This IAE is expressed as [55]:

$$IAE = \int_0^{t_{sim}} |e| \, dt \tag{29}$$

where t_{sim} denotes to the total simulation time, and e is the output deviation, which represents the difference between the desired reference trajectory x_r and actual output x_1. The reference trajectory is set to $cos(t)$. Table 2 shows the values for the design parameters of SMC_{tah} and SMC_{sat}.

Table 2. Optimal value of configuration parameters

Controller	Parameters	Values
SMC_{tah}	a_{tah}	14.8
	k_{tah}	160.3
SMC_{sat}	a_{sat}	31.4
	k_{sat}	152.7
	∅	0.2

5.1. Normal Operation

This simulation is to evaluate the performance of the two controllers in normal operation. Fig. 2 and Fig. 3 show the response and tracking error of the position for the two controlled systems, correspondingly. Table 3 shows the equivalent numerical values for the IAE. Fig. 2 and Fig. 3 show that the SMCtah outperforms the SMCsat. This finding can be validated numerically using Table 3, which clearly shows that the value of and IAE (1.69) for SMCtah is less than the value (1.85) for SMCsat. On other words, the IAE of the system controlled by the SMC_{tah} is reduced by 8.6% compared to that of the system controlled by the SMC_{sat}.

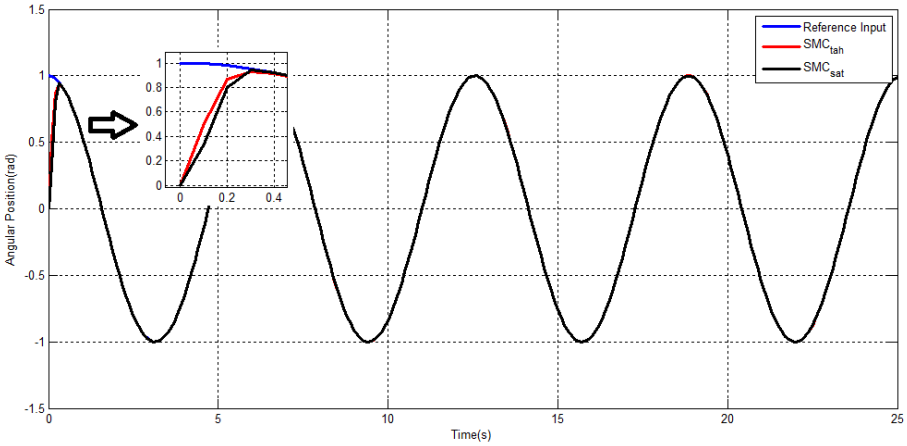

Fig. 2. System response of SMC_{tah} and SMC_{sat} under normal operation

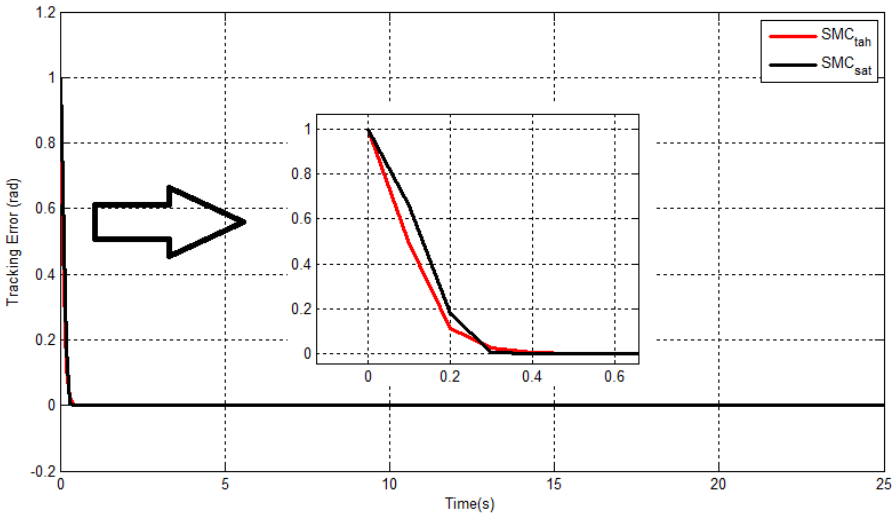

Fig. 3. Tracking error of SMC_{tah} and SMC_{sat} under normal operation

Table 3. Comparison of dynamic performance under normal operation

Performance	SMC_{tah}	SMC_{sat}
IAE	1.69	1.84

5.2. Uncertainty

To examine the ability of the two structures of the SMC to handle the uncertainty, it was assumed that the value of the coefficient A of the Duffing oscillator is increased by 20% of its value. Fig. 4 depicts the response of the two controlled systems. Table 4 gives the numerical values of the IAE for this case. Table 4 illustrates that the value of the IAE for the SMC_{tah} is affected more than the value of the SMC_{sat} as compared to the normal scenario. The IAE of the SMC_{tah} and SMC_{sat} (in the case of increasing the coefficient A of the Duffing oscillator by 20%) is increased by 7.65% and 0.54%, respectively, the as compared to the value of the IAE of the normal scenario.

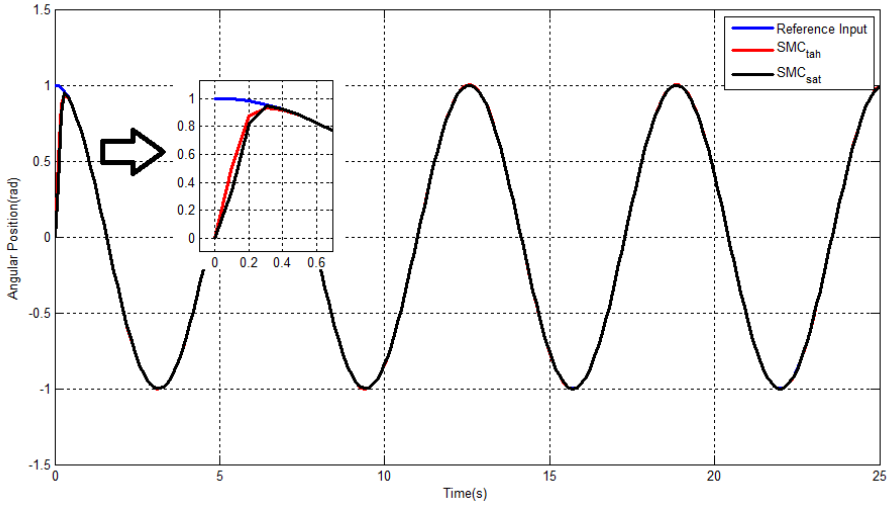

Fig. 4. System response of SMC_{tah} and SMC_{sat} (20% increases in A)

Table 4. Comparison of dynamic performance under uncertainty (20% increases in A)

Performance	SMC_{tah}	SMC_{sat}
IAE	1.83	1.85

Moreover, it was assumed that the value of the coefficient b of the Duffing oscillator is decreased by 20% of its value. Fig. 5 depicts the response of the two controlled systems. Table 5 gives the numerical values of the IAE for this case. Table 5 illustrates that the value of the IAE for the SMC_{tah} is affected more than the value of the SMC_{sat} as compared to the normal scenario. The IAE of the SMC_{tah} and SMC_{sat} (in the case of decreasing the coefficient b of the Duffing oscillator by 20%) is increased by 2.3% and 1.07%, respectively, the as compared to the value of the IAE of the normal scenario.

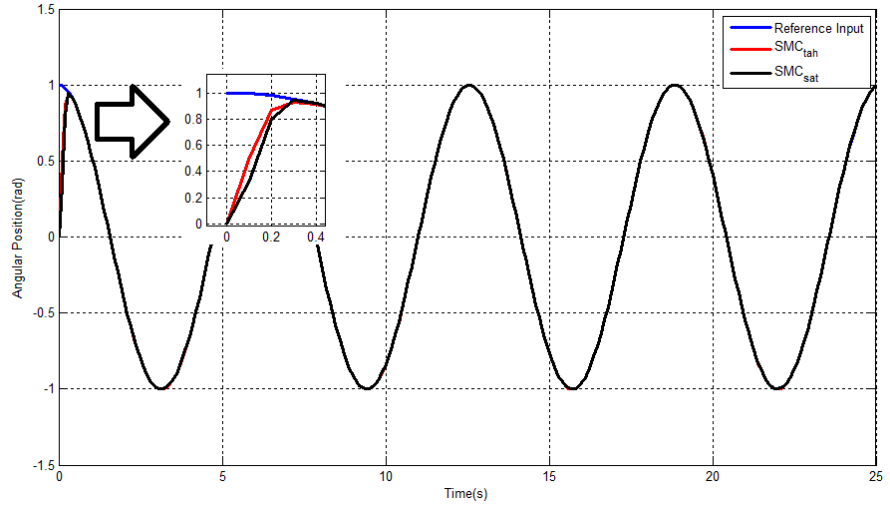

Fig. 5. System response of SMC_{tah} and SMC_{sat} (20% decreases in b)

Table 5. Comparison of dynamic performance under uncertainty (20% decreases in b)

Performance	SMC_{tah}	SMC_{sat}
IAE	1.73	1.86

According to these two scenarios under parameter variation, it can be observed that the SMC_{sat} offers a favourable balance, preserving robustness that closely approximates ideal SMC behaviour while effectively reducing chattering. In contrast, while the SMC_{tah} provides a notably smoother performance, it may entail a modest reduction in robustness—particularly in scenarios involving uncertainties.

6. Conclusion

In this paper a sliding mode controller (SMC) for a Duffing oscillator was proposed. The hyperbolic tangent function (SMC_{tah}) and the saturation function (SMC_{sat}) were used to force the state to slide along the switching manifold. The computer simulation results firstly prove the effectiveness of the proposed controller for trajectory tracking for sinusoidal input. Secondly, the SMC_{tah} show better performance than the SMC_{sat} in terms of reducing the tracking error. Based on the integral of absolute error (IAE), the results data shows that the value of and IAE for SMC_{tah} is 1.69 which is less than the value for SMC_{sat} (1.85). However, the SMC_{sat} exhibits better robustness against parameter uncertainty than SMC_{tah}. Future work may consider the use of different optimization techniques for the SMC parameter tuning, as well as the integration of the adaptive schemes within the SMC structure to achieve an improved performance.

Author Contribution: All authors contributed equally to the main contributor to this paper. All authors read and approved the final paper.

Conflicts of Interest: The authors declare no conflict of interest.

References

[1] J. H. Hung, W. Gao, and J. C. Hung, "Variable structure control: A survey," *IEEE Transactions on Industrial Electronics*, vol. 40, no. 1, pp. 2–22, 1993, https://doi.org/10.1109/41.184817.

[2] E. A. Gedefaw, N. B. Abera, and C. M. Abdissa, "A Review of Modeling and Control Techniques for Unmanned Aerial Vehicles," *Engineering Reports*, vol. 7, no. 6, p. e70215, 2025, https://doi.org/10.1002/eng2.70215.

[3] A. Sabanovic, "Variable structure systems with sliding modes in motion control: A survey," *IEEE Transactions on Industrial Informatics*, vol. 7, no. 2, pp. 212–223, 2011, https://doi.org/10.1109/TII.2011.2123907.

[4] S. V. Emel'yanov, *Sistemy avtomaticheskogo upravleniya s peremennoy strukturoy* [*Automatic control systems with variable structure*]. Moscow, USSR: Nauka Publishing House, Main Editorial Office of Physical and Mathematical Literature, 1967, https://books.google.co.id/books?id=rsqyzgEACAAJ.

[5] V. I. Utkin, "Variable structure systems with sliding modes," *IEEE Transactions on Automatic Control*, vol. 22, no. 2, pp. 212–222, 1977, https://doi.org/10.1109/TAC.1977.1101446.

[6] B. Draženović, "The invariance conditions in variable structure systems," *Automatica*, vol. 5, no. 3, pp. 287–295, 1969, https://doi.org/10.1016/0005-1098(69)90071-5.

[7] N. F. Al-Muthairi and M. Zribi, "Sliding mode control of a magnetic levitation system," *Mathematical Problems in Engineering*, vol. 2004, no. 2, pp. 93–107, 2004, https://doi.org/10.1155/S1024123X04310033.

[8] A. K. Ahmed and H. Al-Khazraji, "Optimal control design for propeller pendulum systems using gorilla troops optimization," *Journal Européen des Systèmes Automatisés*, vol. 56, no. 4, pp. 575–582, 2023, https://doi.org/10.18280/jesa.560407.

[9] A. F. Hasan, M. Nawfal, A. S. Al-Araji, H. Al-Khazraji, and A. J. Humaidi, "Improved sliding mode control for maximum power point tracking in solar photovoltaic applications under varying conditions," *International Journal of Robotics and Control Systems*, vol. 5, no. 3, pp. 1790–1807, 2025, https://doi.org/10.31763/ijrcs.v5i3.1925.

[10] A. Ma'arif, M. A. Marquez Vera, M. S. Mahmoud, E. Umoh, A. J. Abougarair, and S. N. Rahmadhia, "Sliding mode control design for magnetic levitation system," *Journal of Robotics and Control*, vol. 3, no. 6, pp. 848–851, 2022, https://doi.org/10.18196/jrc.v3i6.12389.

[11] C.-Y. Su and T.-P. Leung, "A sliding mode controller with bound estimation for robot manipulators," *IEEE Transactions on Robotics and Automation*, vol. 9, no. 2, pp. 208–214, 1993, https://doi.org/10.1109/70.238284.

[12] M.-S. Park and D. Chwa, "Swing-up and stabilization control of inverted-pendulum systems via coupled sliding-mode control method," *IEEE Transactions on Industrial Electronics*, vol. 56, no. 9, pp. 3541–3555, 2009, https://doi.org/10.1109/TIE.2009.2012452.

[13] B. K. Bose, "An adaptive hysteresis-band current control technique of a voltage-fed PWM inverter for machine drive system," *IEEE Transactions on Industrial Electronics*, vol. 37, no. 5, pp. 402–408, 1990, https://doi.org/10.1109/41.103436.

[14] C. Edwards and S. K. Spurgeon, *Sliding Mode Control: Theory and Applications*. Boca Raton, FL, USA: CRC Press, 1998, https://doi.org/10.1201/9781498701822.

[15] Y. Shtessel, C. Edwards, L. Fridman, and A. Levant, *Sliding Mode Control and Observation*. New York, NY, USA: Springer, 2014, https://doi.org/10.1007/978-0-8176-4893-0.

[16] R. A. DeCarlo, S. H. Zak, and G. P. Matthews, "Variable structure control of nonlinear multivariable systems," *Proceedings of the IEEE*, vol. 76, no. 3, pp. 212–232, 1988, https://doi.org/10.1109/5.4400.

[17] G. Bartolini, "Chattering phenomena in discontinuous control systems," *International Journal of Systems Science*, vol. 20, no. 12, pp. 2471–2481, 1989, https://doi.org/10.1080/00207728908910327.

[18] W. Gao and J. Hung, "Variable structure control of nonlinear systems: A new approach," *IEEE Transactions on Industrial Electronics*, vol. 40, no. 1, pp. 45–55, 1993, https://doi.org/10.1109/41.184820.

[19] L. Tao, Q. Chen, Y. Nan, and C. Wu, "Double hyperbolic reaching law with chattering-free and fast convergence," *IEEE Access*, vol. 6, pp. 27717–27723, 2018, https://doi.org/10.1109/ACCESS.2018.2838127.

[20] P. Latosiński, "Sliding mode control based on the reaching law approach: A brief survey," in *Proceedings of the IEEE International Conference on Control*, 2017, pp. 519–523, https://doi.org/10.1109/MMAR.2017.8046882.

[21] J. Wu, Y. Wang, W. Zhang, Z. Nie, R. Lin, and H. Ma, "Defect detection of pipes using Lyapunov dimension of Duffing oscillator based on ultrasonic guided waves," *Mechanical Systems and Signal Processing*, vol. 82, pp. 130–147, 2017, https://doi.org/10.1016/j.ymssp.2016.05.012.

[22] A. Hashmi, M. F. Hanif, and A. I. Bhatti, "Simulation and analysis of Duffing oscillator using sliding mode control," in *Proceedings of the 2017 International Conference on Communication, Computing and Digital Systems (C-CODE)*, 2017, pp. 326–330, https://doi.org/10.1109/C-CODE.2017.7918951.

[23] N. X. Chiem, T. C. Phan, P. D. Thai, and B. X. Hai, "Implementation of a synergetic controller for a 2-DOF helicopter on an embedded platform using an STM32 microcontroller," *Buletin Ilmiah Sarjana Teknik Elektro*, vol. 7, no. 2, pp. 253–269, Jul. 2025, http://journal2.uad.ac.id/index.php/biste/article/view/13410.

[24] A. Abdullah, H. Ali, A. Al-Qassar, and S. Al-Samarraie, "Comparative analysis of two robust strategies for an angular velocity control system," *Iraqi Journal of Computers, Communications, Control and Systems Engineering*, vol. 24, no. 3, pp. 86–103, 2024, https://doi.org/10.33103/uot.ijccce.24.3.7.

[25] A. S. Al-Khayyat, A. A. Ouda, and M. J. Hameed, "Airflow rate control of oscillating water column for maximising wave energy capture," *e-Prime – Advances in Electrical Engineering, Electronics and Energy*, vol. 12, p. 100963, 2025, https://doi.org/10.1016/j.prime.2025.100963.

[26] M. A. Al-Ali, O. F. Lutfy, and H. Al-Khazraj, "Investigation of optimal controllers on dynamics performance of nonlinear active suspension systems with actuator saturation," *Journal of Robotics and Control (JRC)*, vol. 5, no. 4, pp. 1041–1049, 2024, https://journal.umy.ac.id/index.php/jrc/article/view/22139.

[27] A. Sarwat, W. Lu, and M. Iqbal, "Nonlinear control of a fully actuated robotic hand using high-order sliding mode and feedback linearization controllers," *PLoS One*, vol. 20, no. 10, p. e0333512, 2025, https://doi.org/10.1371/journal.pone.0333512.

[28] N. Q. Yousif, S. S. Husain, O. H. Abdullah, A. J. Humaidi, and A. K. Al-Mhdawi, "Rise control design to reduce earthquake effect on building structures with MRD," *Journal of Engineering Science and Technology*, vol. 20, no. 5, pp. 1568–1581, 2025, https://jestec.taylors.edu.my/Vol%2020%20Issue%205%20Octorber%202025/20_5_19.pdf.

[29] A. M. Abdullah, H. M. Ali, and A. A. Al-Qassar, "A robust controller design for an inlet throttling speed control system for a rotary actuator," *International Journal of Mechatronics and Applied Mechanics*, vol. 2024, no. 15, pp. 179–188, 2024, https://ijomam.com/wp-content/uploads/2024/03/pag.-179-188_A-ROBUST-CONTROLLER-DESIGN-FOR-AN-INLET-THROTTLING-SPEED-CONTROL-SYSTEM-FOR-A-ROTARY-ACTUATOR.pdf.

[30] P. Jekan, R. Dharshini, R. Mohith, and A. Swathi, "Design of robust controller for ball and beam," in *Proceedings of the 2025 IEEE International Students' Conference on Electrical, Electronics and Computer Science (SCEECS)*, 2025, pp. 1–8, https://doi.org/10.1109/SCEECS64059.2025.10941125.

[31] A. L. Shuraiji and S. W. Shneen, "Analysis of improved performance and dynamics of an induction motor using an artificial neural network controller and a conventional proportional–integral–derivative controller," *Buletin Ilmiah Sarjana Teknik Elektro*, vol. 7, no. 3, pp. 397–408, 2025, https://journal2.uad.ac.id/index.php/biste/article/view/13820.

[32] B. Nawress, A. N. Gharbi, and N. B. Braiek, "Sliding mode control based on neural state and disturbance observers: Application to a unicycle robot using ROS2," *Journal of Robotics and Control*, vol. 5, no. 4, pp. 964–980, 2024, https://journal.umy.ac.id/index.php/jrc/article/view/21650/9186.

[33] Y. Soufi, S. Kahla, and M. Bechouat, "Particle swarm optimization based sliding mode control of variable speed wind energy conversion system," *International Journal of Hydrogen Energy*, vol. 41, no. 45, pp. 20956–20963, 2016, https://doi.org/10.1016/j.ijhydene.2016.05.142.

[34] A. R. Laware, D. B. Talange, and V. S. Bandal, "Design of predictive sliding mode controller for cascade control system," in *Proceedings of the 2016 IEEE First International Conference on Control, Measurement and Instrumentation*, 2016, pp. 284–289, https://doi.org/10.1109/CMI.2016.7413756.

[35] R. Xu and U. Ozguner, "Sliding mode control of a quadrotor helicopter," in *Proceedings of the 45th IEEE Conference on Decision and Control*, 2006, pp. 4957–4962, https://doi.org/10.1109/CDC.2006.377588.

[36] A. M. Hameed and A. K. Hamoudi, "A 2-link robot with adaptive sliding mode controlled by barrier function," *Journal Européen des Systèmes Automatisés*, vol. 56, no. 6, p. 1105, 2023, https://doi.org/10.18280/jesa.560620.

[37] H. Jin and X. Zhao, "Approach angle-based saturation function of modified complementary sliding mode control for permanent magnet linear synchronous motor," *IEEE Access*, vol. 7, pp. 126014–126024, 2019, https://doi.org/10.1109/ACCESS.2019.2939140.

[38] S. Khlil, H. Al-Khazraji, and Z. Alabacy, "Solving assembly production line balancing problem using greedy heuristic method," *IOP Conference Series: Materials Science and Engineering*, vol. 745, no. 1, pp. 1–7, 2020, https://doi.org/10.1088/1757-899X/745/1/012068.

[39] A. Uzzaman, M. Islam, and S. Ahmed, "Bio-inspired hybrid control for autonomous vehicles: Improving real-time navigation through the integration of ACO and PSO," *Control Systems and Optimization Letters*, vol. 3, no. 3, pp. 234–240, 2025, https://ejournal.csol.or.id/index.php/csol/article/view/204/192.

[40] M. Alrashed and M. Elnaggar, "Enhanced DC-link voltage stability in grid-connected PV systems via three recent metaheuristic optimizers: Towards high penetration of PV systems in modern power systems," *International Journal of Robotics and Control Systems*, vol. 5, no. 6, pp. 2709–2728, 2025, https://pubs2.ascee.org/index.php/IJRCS/article/view/2224/pdf.

[41] S. Tahcfulloh, D. Maulianawati, and D. Wiharyanto, "Optimizing 2.4 GHz wireless networks in shrimp ponds with particle swarm optimization," *Jurnal Ilmiah Teknik Elektro Komputer dan Informatika*, vol. 10, no. 4, pp. 817–832, 2024, https://journal.uad.ac.id/index.php/JITEKI/article/view/30236/12820.

[42] P. Sarker, A. Ksibi, M. M. Jamjoom, K. Choi, A. A. Nahid, and M. A. Samad, "Breast cancer prediction with feature-selected XGB classifier optimized by metaheuristic algorithms," *Journal of Big Data*, vol. 12, no. 1, p. 78, 2025, https://doi.org/10.1186/s40537-025-01132-7.

[43] A. I. Abdulkareem, H. Abd Dhahad, and N. Q. Yousif, "Prospect theory in particle swarm optimization for constrained nonlinear optimization problems," in *Proceedings of the 2018 Third Scientific Conference of Electrical Engineering*, 2018, pp. 144–149, https://doi.org/10.1109/SCEE.2018.8684144.

[44] R. M. Naji, H. Dulaimi, and H. Al-Khazraji, "An optimized PID controller using enhanced bat algorithm in drilling processes," *Journal Européen des Systèmes Automatisés*, vol. 57, no. 3, pp. 767–772, 2024, https://doi.org/10.18280/jesa.570314.

[45] F. R. Yaseen and H. Al-Khazraji, "Optimized vector control using swarm bipolar algorithm for five-level PWM inverter-fed three-phase induction motor," *International Journal of Robotics and Control Systems*, vol. 5, no. 1, pp. 333–347, 2025, https://doi.org/10.31763/ijrcs.v5i1.1713.

[46] A. F. Hasan, H. A. Raheem, and R. Hussein, "Performance improvement of manipulator actuated by pneumatic artificial muscles based on synergetic control and social spider optimization algorithm," *Acta Polytechnica*, vol. 64, no. 6, pp. 519–529, 2024, https://doi.org/10.14311/AP.2024.64.0519.

[47] S. Mirjalili and A. Lewis, "The whale optimization algorithm," Advances in Engineering Software, vol. 95, pp. 51–67, 2016, https://doi.org/10.1016/j.advengsoft.2016.01.008.

[48] I. Aljarah, H. Faris, and S. Mirjalili, "Optimizing connection weights in neural networks using the whale optimization algorithm," Soft Computing, vol. 22, no. 1, pp. 1–15, 2018, https://doi.org/10.1007/s00500-016-2442-1.

[49] Q. V. Pham, S. Mirjalili, N. Kumar, M. Alazab, and W. J. Hwang, "Whale optimization algorithm with applications to resource allocation in wireless networks," *IEEE Transactions on Vehicular Technology*, vol. 69, no. 4, pp. 4285–4297, 2020, https://doi.org/10.1109/TVT.2020.2973294.

[50] R. Masadeh, A. Alzaqebah, and A. Sharieh, "Whale optimization algorithm for solving the maximum flow problem," *Journal of Theoretical & Applied Information Technology*, vol. 96, no. 8, pp. 2208–2220, 2018, https://easychair.org/publications/preprint/FvqZ.

[51] Q. Han, X. Yang, H. Song, S. Sui, H. Zhang, and Z. Yang, "Whale optimization algorithm for ship path optimization in large-scale complex marine environment," *IEEE Access*, vol. 8, pp. 57168–57179, 2020, https://doi.org/10.1109/ACCESS.2020.2982617.

[52] F. R. Yaseen, M. Q. Kadhim, H. Al-Khazraji, and A. J. Humaidi, "Decentralized control design for heating system in multi-zone buildings based on whale optimization algorithm," *Journal Européen des Systèmes Automatisés*, vol. 57, no. 4, pp. 981–989, 2024, https://doi.org/10.18280/jesa.570406.

[53] N. C. Patel and M. K. Debnath, "Whale optimization algorithm tuned fuzzy integrated PI controller for load frequency control problem in thermal–hydro–wind interconnected system," in *Applications of Computing, Automation and Wireless Systems in Electrical Engineering: Proceedings of MARC*, 2018, pp. 67–77, https://doi.org/10.1007/978-981-13-6772-4_7.

[54] M. Thanoon, M. Almaged, and A. Abdulla, "Boost converter control using proportional–integral–derivative controller optimized by whale optimization algorithm," *International Journal of Robotics and Control Systems*, vol. 5, no. 3, pp. 1850–1865, 2025, https://doi.org/10.31763/ijrcs.v5i3.1912.

[55] R. A. Mahmod, R. A. Kadhima, M. Nawfal, and H. Al-Khazraji, "High-gain observer-based backstepping control design for nonlinear single-axis driven systems," *International Journal of Robotics and Control Systems*, vol. 5, no. 3, pp. 1886–1899, 2025, https://doi.org/10.31763/ijrcs.v5i3.1984.